SCHOLARLY PUBLICATIONS
School of Applied Sciences
KIIT Deemed to be University

Journal Name: Journal of Materials Chemistry C **IF: 6.4**

Title: Morphological evolution of individual microrods to self-assembled 3D hierarchical flower architectures of CuBixIn1-xSe2 for photo response applications

Author: Priyadarshini, Priyanka; Senapati, Subrata; Mohapatra, Ashutosh; Pradhan, Monalisa; Alagarasan, Devarajan; Naik, Ramakanta

Details: February 2024

Abstract: CuInSe2 and CuInGaSe2 are extremely promising materials for solar cell applications, wherein bandgap shrinkage is highly desirable for manufacturing transparent/semitransparent layers. In this work, this shrinkage was achieved by replacing In with Bi, and the change in current-voltage responses for photodetector applications was further studied. CuBixIn1-xSe2 microrod (MR) flowers (x = 0, 0.2, 0.4, 0.6, and 0.8) were synthesized via microwave synthesis using different Bi/In concentrations. The variation in the composition of Bi/In caused alteration in structural, morphological, and optical behaviors. CuInSe2 showed a polycrystalline nature, while Bi incorporation led to the appearance of a Bi2Se3 phase. Raman peaks corresponding to different vibrational bonds shifted with change in Bi/In content, indicating that the composition variation induced structural transformation inside the matrix. Morphological analysis showed a transition from MRs to MR-based flowers with the introduction of bismuth. Optical absorption was enhanced with an increase in Bi content due to a change in the MR size, forming a flower-like architecture. This reduced the optical bandgap by increasing defects and disorders in the forbidden gap. At 532 nm excitation, broad photoluminescence band emission was observed for all samples. Each spectrum showed three deconvoluted peaks, which were attributed to a transition among localized states over the forbidden gap region. The MRs demonstrated good photo response towards white light. Their photocurrent reduced from the mu A to the nA range with varying compositions. The observed optical and electrical properties of the MRs are most suitable for various optoelectronic device applications.

URL: https://pubs.rsc.org/en/content/articlelanding/2024/tc/d3tc03250g

SCHOLARLY PUBLICATIONS
School of Applied Sciences
KIIT Deemed to be University

Journal Name: Journal of Materials Chemistry **IF: 6.4**

Title: Morphological evolution of individual microrods to self-assembled 3D hierarchical flower architectures of CuBixIn1−xSe2 for photo response applications

Author: Priyadarshini P., Senapati S., Mohapatra A., Pradhan M., Alagarasan D., Naik R.

Details: Volume 12, Issue 8, Pages 2879 – 2893, 15 January 2024

Abstract: $CuInSe_2$ and $CuInGaSe_2$ are extremely promising materials for solar cell applications, wherein bandgap shrinkage is highly desirable for manufacturing transparent/semitransparent layers. In this work, this shrinkage was achieved by replacing In with Bi, and the change in current-voltage responses for photodetector applications was further studied. $CuBi_xIn_{1-x}Se_2$ microrod (MR) flowers (x = 0, 0.2, 0.4, 0.6, and 0.8) were synthesized via microwave synthesis using different Bi/In concentrations. The variation in the composition of Bi/In caused alteration in structural, morphological, and optical behaviors. $CuInSe_2$ showed a polycrystalline nature, while Bi incorporation led to the appearance of a Bi_2Se_3 phase. Raman peaks corresponding to different vibrational bonds shifted with change in Bi/In content, indicating that the composition variation induced structural transformation inside the matrix. Morphological analysis showed a transition from MRs to MR-based flowers with the introduction of bismuth. Optical absorption was enhanced with an increase in Bi content due to a change in the MR size, forming a flower-like architecture. This reduced the optical bandgap by increasing defects and disorders in the forbidden gap. At 532 nm excitation, broad photoluminescence band emission was observed for all samples. Each spectrum showed three deconvoluted peaks, which were attributed to a transition among localized states over the forbidden gap region. The MRs demonstrated good photo response towards white light. Their photocurrent reduced from the μA to the nA range with varying compositions. The observed optical and electrical properties of the MRs are most suitable for various optoelectronic device applications.

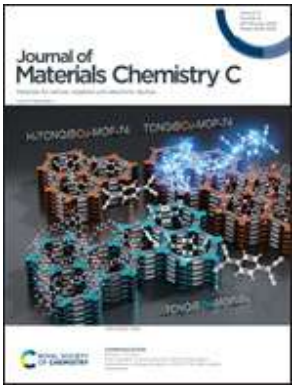

URL: https://pubs.rsc.org/en/content/articlelanding/2024/tc/d3tc03250g

SCHOLARLY PUBLICATIONS
School of Applied Sciences
KIIT Deemed to be University

Journal Name: Journal of Alloys and Compound **IF: 6.2**

Title: Tailoring optical properties of hydrothermally synthesized SnMnSe nanocubes for optoelectronic and dielectric application

Author: Abinash Parida , Subrata Senapati , Gopal K. Pradhan & Ramakanta Naik

Details: Volume 970 , January 2024

Abstract: In the current paper, we investigate the optical and dielectric properties of the SnMnSe nanocubes. The $Sn_{0.5+x}Mn_{0.5-x}Se$ (x = 0.375, 0.250, 0.125, 0) samples are prepared by simple hydrothermal method with the variation of the Sn and Mn concentration. The X-ray diffraction study shows that all the prepared samples are polycrystalline in nature. The average crystallite size increases along with the dislocation density and the average strain value with the increase in the Mn concentration. The morphology shows the formation of nanocubes. The average size of the cubes increases with the increase of Mn content. The reflectance data demonstrate the decreasing order of absorption edges with the increase of Mn content in the sample. The variation of the absorption edges with Mn content tends to decrease the optical bandgap by creating more disorder and defects between the gap region. Broad orange-red photoluminescence emission is observed for all the samples with 532 nm excitation. The electrical study of the sample shows high resistance values. The dielectric behavior as a function of frequency and temperature is investigated, and parameters like dielectric constant, AC conductivity, impedance spectroscopy, and electric modulus are deeply analyzed. The dielectric properties are useful for energy storage applications. All the above optical and dielectric properties of the SnMnSe matrix have potential use in the field of optoelectronics and dielectric applications.

URL: https://www.sciencedirect.com/science/article/pii/S0925838823038239?via%3Dihub

SCHOLARLY PUBLICATIONS
School of Applied Sciences
KIIT Deemed to be University

Journal Name : Journal of Alloys and Compounds **I.F: 6.2**

Title: Optimization of (Ba1−xCax)(Ti0.9Sn0.1)O3 ceramics in X-band using Machine Learning

Author: Dikshit A.P., Das D., Samal R.R., Parashar K., Mishra C., Parashar S.K.S.

Details: Volume 982, 30 April 2024 , Article number 173797

Abstract: Developing efficient electromagnetic interference shielding materials has become significantly important in present times. This paper reports a series of $(Ba_{1-x}Ca_x)(Ti_{0.9}Sn_{0.1})O_3$ (BCTS) (x=0,0.01,0.05,0.1) ceramics synthesized by conventional method which were studied for electromagnetic interference shielding (EMI) applications in X-band (8–12.4 GHz). EMI shielding properties and all S parameters (S_{11} & S_{12}) of BCTS ceramic pellets were measured in the frequency range (8–12.4 GHz) using a Vector Network Analyser (VNA). The BCTS ceramic pellets for x = 0.05 showed maximum total effective shielding of 46 dB indicating good shielding behaviour for high-frequency applications. However, the development of lead-free ceramics with different concentrations usually requires iterative experiments resulting in, longer development cycles and higher costs. To address this, we used a machine learning (ML) strategy to predict the EMI shielding for different concentrations and experimentally verify the concentration predicted to give the best EMI shielding. The ML model predicted BCTS ceramics with concentration (x = 0.06, 0.07, 0.08, and 0.09) to have higher shielding values. On experimental verification, a shielding value of 58 dB was obtained for x = 0.08, which was significantly higher than what was obtained experimentally before applying the ML approach. Our results show the potential of using ML in accelerating the process of optimal material development, reducing the need for repeated experimental measures significantly.

URL: https://www.sciencedirect.com/science/article/pii/S0925838824003839?via%3Dihub

SCHOLARLY PUBLICATIONS
School of Applied Sciences
KIIT Deemed to be University

Journal Name: ACS Applied Nano Materials **IF: 5.9**

Title: No-Stirring Synthesis of sub-50 nm Hollow Silver Nanoshells with Dimethylglyoxime-Induced Plasmons in Visible and Second NIR Windows for Biomedical Applications

Author: Dadhich B.K., Gupta P., Ballav S., Bhushan B., Datta P.K., Priyam A.

Details: Volume 7, Issue 1, Pages 1212 – 1221, 12 January 2024

Abstract: A unique no-stirring synthesis has been developed to obtain highly monodisperse hollow silver nanoshells (HAgNSs) with plasmons in the second near-IR (NIR-II) window. The method also introduces dimethylglyoxime (DMG) as a quadrupole-supporting agent. The quadrupole surface plasmon resonance (Q-SPR) was found to be highly intense and tunable from 450 to 558 nm. Two types of dipolar resonances, symmetric dipole surface plasmon resonance (SD-SPR) and antisymmetric dipole surface plasmon resonance (AD-SPR), are also observed. The AD-SPR peaks remain constant at 333 nm while the SD-SPR peaks are tuned gradually from 780 to 850 → 920 → 1000 → 1150 nm. They were accordingly named HAgNS-780, HAgNS-850, HAgNS-920, HAgNS-1000, and HAgNS-1150, and their outer diameters were found to be 53 ± 4, 49 ± 3, 54 ± 3, 62 ± 5, and 39 ± 3 nm, respectively. The corresponding aspect ratios (outer diameter/shell thickness) were 3.31, 3.37, 3.48, 4.13, and 5.2, respectively. A correlation between the tunability of SD-SPR, AD-SPR, and Q-SPR and aspect ratio has been established. The shape and size parameters were utilized for the simulation of the extinction spectra by the discrete dipole approximation (DDA) method. Second derivative FTIR analysis reveals the peculiar binding mode of DMG to the HAgNS which is the genesis of Q-SPR in such smaller-sized nanoshells. The further red shift of Q-SPR and SD-SPR was observed with the addition of folic acid (FA). It also imparts greater aqueous solubility, colloidal stability, and biocompatibility, making them suitable for biomedical applications.

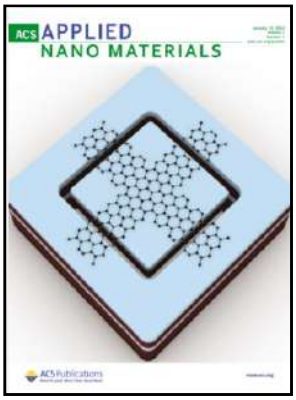

URL: https://pubs.acs.org/doi/10.1021/acsanm.3c05191

SCHOLARLY PUBLICATIONS
School of Applied Sciences
KIIT Deemed to be University

Journal Name: Polymer Composites **IF: 5.2**

Title: Fabrication of Multiwalled Carbon Nanotubes (MWCNT) and Reduced Graphene Oxide (rGO)-based thermoplastic polyurethane and polypyrrole nanocomposites for electromagnetic wave absorption application with a low reflection

Author: Acharya Swatee, Swain Lopa Mudra, Samal Ritu Roumya, Parashar S. K. S, Sahoo Bibhu Pras

Details: 22 December 2023

Abstract: Electromagnetic radiation (EMR) pollution is a serious concern in today's environment, causing problems not just for electronic gadgets but also for living society. The goal of this research is to fabricate thermoplastic polyurethane (TPU) and polypyrrole (PPy)-based 95:5 blend nanocomposites using a simple solvent casting method at such a low concentration of rGO and MWCNT (0.3, 0.4, 0.5 php) (parts per hundred polymers), for electromagnetic wave (EMW) absorption applications. The chemical interaction between the different phases and morphology of the nanocomposites is characterized by Raman spectroscopy, X-ray diffraction (XRD), and field emission scanning electron microscopy (FESEM) techniques. The material properties, such as dielectric and magnetic properties, are analyzed in X-band frequency (8.2–12.4 GHz). The total shielding effectiveness of (SETot) 0.5 rGO system is found to be 27 dB, whereas, for corresponding MWCNT nanocomposites, it is 26 dB. Interestingly, in 0.5 rGO nanocomposites, absorption shielding effectiveness (SEAbs) is approximately 25 dB, and reflection shielding effectiveness (SERef) is less than 2 dB, which indicates the absorption of 70% of the electromagnetic wave, and the rest gets reflected. Apart from that, the rGO-based nanocomposites possess a greater extent of thermal stability than the corresponding MWCNT-based nanocomposites.

URL: https://4spepublications.onlinelibrary.wiley.com/doi/10.1002/pc.28027?af=R

Journal Name: Ceramics International **IF: 5.2**

Title: Structural, relaxor behavior, and energy storage performance of BaTiO3-Bi (Mg2/3Nb1/3)O3 solid solutions for potential MLCC application

Author: Sahoo, S.; Badapanda, T.; Kumar, D.; Rout, S. K.; Mohanty, S.; Ray, J.; Tripathy, Satya N.

Details: Volume 49,Issue 23 Part A, December 2023, Pages 37700-37711

Abstract: In the discussed work, (1-x) BaTiO3 (BT)-x Bi(Mg2/3Nb1/3)O3 (BMN) solid-combinations have been synthesized via the solid-state process; and both corresponding dielectric and ferroelectric behavior have been learned for possible Multilayer Ceramic Capacitor (MLCC) applications. The phase confirmation has been identified utilizing X-ray diffraction; and Rietveld refinement technique has been used for structural analysis that unveils the formation of pure perovskite structure of the prepared ceramics. Rietveld refinement results reveal the structural changeover from tetragonal to pseudo-cubic for x≥0.125. Raman spectroscopy measurements confirm the structural phase changes and lattice modifications due to the chemical substitutions. Microstructural analysis has been done with the help of electron micrograph. Dielectric performance of the synthesized (1-x)BaTiO3(BT)-xBi(Mg2/3Nb1/3)O3(BMN) solid solutions has been examined within a temperature range of 173K–473K at different applied frequencies. A broad phase transition and relaxor character is detected from dielectric investigation. The relaxor behavior has been quantified by the Vogel-Fulcher fitting. The thermal stability of the prepared samples was calculated by means of standard formula of Temperature Coefficient of Capacitance (TCC). Hysteresis loop was undertaken to identify the ferroelectric properties and energy storage capacity. Among all the compositions, x = 0.10 shows good thermal stability, an elevated recoverable energy density; and a remarkable efficiency that makes it suitable for MLCC applications.

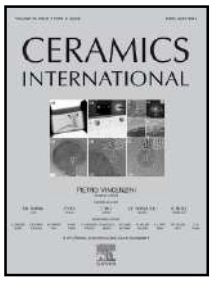

URL: https://www.sciencedirect.com/science/article/pii/S0272884223027190?via%3Dihub

SCHOLARLY PUBLICATIONS
School of Applied Sciences
KIIT Deemed to be University

Journal Name: Journal of Biomolecular Structure and Dynamics **IF: 4.4**

Title: In silico screening of phytoconstituents as potential anti-inflammatory agents targeting NF-κB p65: an approach to promote burn wound healing

Author: Pattnaik, Saswati; Murmu, Sneha; Rath, Bibhu Prasad; Singh, Mahender Kumar; Kumar, Sunil; Mohanty, Chandana

Details: 29 January 2024

Abstract: Chronic burn wounds are frequently characterised by a prolonged and dysregulated inflammatory phase that is mediated by over-activation of NF-κB p65. Synthetic wound healing drugs used for treatment of inflammation are primarily associated with several shortcomings which reduce their therapeutic index. In this scenario, phytoconstituents that exhibit multifaceted biological activities including anti-inflammatory effects have emerged as a promising therapeutic alternative. However, identification and isolation of phytoconstituents from medicinal herbs is a cumbersome method that is linked to profound uncertainty. Hence, present study aimed to identify prospective phytoconstituents as inhibitors of RHD of NF-κB p65 by utilizing in silico approach. Virtual screening of 2821 phytoconstituents was performed against protein model. Out of 2821 phytoconstituents, 162 phytoconstituents displayed a higher binding affinity (≤ −8.0 kcal/mol). These 162 phytoconstituents were subjected to ADMET predictions, and 15 of them were found to satisfy Lipinski's rule of five and showed favorable pharmacokinetic properties. Among these 15 phytoconstituents, 5 phytoconstituents with high docking scores i.e. silibinin, bismurrayaquinone A, withafastuosin B, yuccagenin, (+)-catechin 3-gallate were selected for molecular dynamics (MD) simulation analysis. Results of MD simulation indicated that withafastuosin B, (+)-catechin 3-gallate and yuccagenin produced a compact and stable complex with protein without significant variations in conformation. Relative binding energy analysis of best hit molecules indicate that withafastuosin B, and (+)-catechin 3-gallate exhibit high binding affinity with target protein among other lead molecules. Findings of study suggest that these phytoconstituents could serve as promising anti-inflammatory agents for treatment of burn wounds by inhibiting the RHD of NF-κB p65.

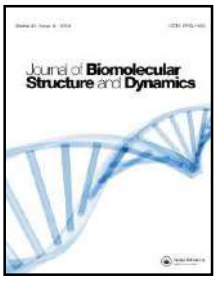

URL: https://www.tandfonline.com/doi/full/10.1080/07391102.2024.2306199

SCHOLARLY PUBLICATIONS
School of Applied Sciences
KIIT Deemed to be University

Journal Name: Biocatalysis and Agricultural Biotechnology **IF: 4.0**

Title: Characterization of halotolerant phosphate-solubilizing rhizospheric bacteria from mangrove (Avicennia sp.) with biotechnological potential in agriculture and pollution mitigation

Author: Gobinda Dey, Jyoti Prakash Maity, Pritam Banerjee, Raju Kumar Sharma, Hassan Etesami, Tapan Kumar Bastia, Prasanta Rath, Uttara Sukul, Hsien-Bin Huang, Kuo-Wei Huang & Chien-Yen Chen.

Details: Volume 55, Article No. 102960, January 2024

Abstract: Mangroves represent intricate and ever-changing ecosystems, exhibiting fluctuations in water level, salinity, and nutrient (such as NPK) availability as well as a wide array of unique bacterial communities. Microbial interactions in different components (e.g., tree roots) of the mangrove ecosystem are crucial to understand the ecosystem functioning for potential application in pollution mitigation and agricultural production. This study aimed to isolate phosphate-solubilizing bacteria (PSB) from the rhizosphere sediment of mangrove (Avicennia sp.) in terms of heavy metals (HMs) and salinity tolerance as well as plant growth promoting (PGP) traits, where the effective PSB were used on Brassica chinensis for their seed priming and growth under salinity stress. The effective two PSB isolates were identified by 16S rRNA, where JKD01 and JKD02 were closely related (99%) to Enterobacter cloacae (OQ271412) and Kocuria rhizophila (OQ271413), respectively. Both the strains exhibited phosphate solubilization, IAA, NH3, and EPS production ability as well as HMs resistant ability where, E. cloacae (OQ271412) and K. rhizophila (OQ271413), are effectively remove the Cu from the water with 33.23% and 27.54%, respectively. The FTIR results showed functional group shifts (carboxyl, phosphate, and amino) in Cu-treated bacterial biomass and intracellular Cu presence, indicating the involvement of Cu in the bio-sorption and intracellular bioaccumulation process, respectively. The findings suggested PSB tolerance to salinity and HMs are present in mangroves, making them a valuable source for isolating effective bacteria to reduce stress in plants, lower HMs accumulation in mangroves, and aid in the bioremediation of HMs-contaminated environments.

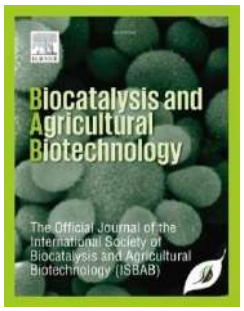

URL: https://www.sciencedirect.com/science/article/abs/pii/S1878818123003614

SCHOLARLY PUBLICATIONS
School of Applied Sciences
KIIT Deemed to be University

Journal Name: Journal of Physics and Chemistry of Solids **IF: 4.0**

Title: Impact of structural distortion on electronic and magnetic properties of La2MnVO6 double perovskite: An ab initio approach

Author: Aiswarya Priyambada & Priyadarshini Parida

Details: Volume 188, Article No. 111892, May 2024

Abstract: We have studied the detailed structural, electronic, and magnetic properties of La_2MnVO_6 double perovskite considering both ab initio and semiempirical parameters within the density functional formalism. We have also considered the strong electron correlation (density functional theory plus the Hubbard potential U) in our calculations to determine the ground state of the compound. Investigation of detailed structural properties with both ab initio and semiempirical parameters reveals that the structure obtained with the semiempirical parameters is more distorted, having more distorted octahedra than the theoretically optimized structure obtained with the variable-cell relaxation method. The stable magnetic phase of the compound is obtained as ferromagnetic with use of the energy minimization principle with the Hubbard potential. Study of the electronic properties shows that the compound is a half-metal with the ab initio parameters, whereas it behaves as a semimetal with the semiempirical parameters. The final ground state of the compound is concluded to be a ferromagnetic metal.

URL: https://www.sciencedirect.com/science/article/pii/S0022369724000271?via%3Dihub

SCHOLARLY PUBLICATIONS
School of Applied Sciences
KIIT Deemed to be University

Journal Name: Scientific Reports **IF: 4.0**

Title: Stronger EPR-steering criterion based on inferred Schrödinger–Robertson uncertainty relation

Author: Rakesh Mohan Das

Details: Volume 14, Issue 1, January 2024

Abstract: Steering is one of the three in-equivalent forms of nonlocal correlations intermediate between Bell nonlocality and entanglement. Schrödinger–Robertson uncertainty relation (SRUR), has been widely used to detect entanglement and steering. However, the steering criterion in earlier works, based on SRUR, did not involve complete inferred-variance uncertainty relation. In this paper, by considering the local hidden state model and Reid's formalism, we derive a complete inferred-variance EPR-steering criterion based on SRUR in the bipartite scenario. Furthermore, we check the effectiveness of our steering criterion with discrete variable bipartite two-qubit and two-qutrit isotropic states.

URL: https://www.nature.com/articles/s41598-023-50029-z

Journal Name: RSC Advances **IF: 3.9**

Title: Recent progress in graphene and its derived hybrid materials for high-performance supercapacitor electrode applications

Author: Sahoo, Prasanta Kumar; Kumar, Niraj; Jena, Anirudha; Mishra, Sujata; Lee, Chuan-Pei; Lee, Seul-Yi; Park, Soo-Jin

Details: Volume 14, Issue 2, 2024, Pages 755- 1526

Abstract: Graphene, the most fascinating 2D form of carbon with closely packed carbon atoms arranged in a layer, needs more attention in various fields. For its unique electrical, mechanical, and chemical properties with a large surface area, graphene has been in the limelight since its first report. Graphene has extraordinary properties, making it the most promising electrode component for applications in supercapacitors. However, the persistent re-stacking of carbon layers in graphene, caused by firm interlayer van der Waals attractions, significantly impairs the performance of supercapacitors. As a result, many strategies have been used to get around the aforementioned problems. The utilization of graphene-based nanomaterials has been implemented to surmount the aforementioned constraints and considerably enhance the performance of supercapacitors. This review highlights recent progress in graphene-based nanomaterials with metal oxide, sulfides, phosphides, nitrides, carbides, and conducting polymers, focusing on their synthetic approach, configurations, and electrochemical properties for supercapacitors. It discusses new possibilities that could increase the performance of next-generation supercapacitors.

URL: https://pubs.rsc.org/en/content/articlelanding/2024/ra/d3ra06904d

SCHOLARLY PUBLICATIONS
School of Applied Sciences
KIIT Deemed to be University

Journal Name: Journal of Molecular Structure **IF: 3.8**

Title: Synthesis, X-ray structures, Hirshfeld surface analysis, and redox behaviour of 2-substituted-1H-perimidine derivatives

Author: Priy anka R. Angarkhe, Aijaz Shaikh, Smruti Rekha Rout, Bipul Sarma, Jagnyaseni Tripathy, Rambabu Dandela & Swagat K. Mohapatra

Details: Volume 1296, Part-1, January 2024

Abstract: Peri-naptho fused pyrimidine derivatives, known as 1H-perimidines or 1H-benzo[d,e]quinazolines, have recently been studied for a diverse range of applications. A series of 2-substituted-1H-perimidine compounds (1A–1F) have been synthesized by the condensation reaction of 1,8-diaminonaphthalene with the appropriate aldehyde. The 2-substituted-1H-perimidinium iodide salts ($1A^+I^-$–$1F^+I^-$) were obtained by methylating 1H-perimidine using methyl iodide in the presence of a mild base K_2CO_3. The perimidinium salts were reduced using $NaBH_4$ in methanol to obtain 2-substituted-2,3-dihydro-1H-perimidine compounds (1AH–1FH). The compounds were characterized by ^1H, ^{13}C-NMR and UV–Vis absorption spectroscopy, elemental analysis, and in the case of compounds 1C, $1B^+I^-$, $1C^+I^-$, $1E^+I^-$, $1F^+I^-$, and 1BH–1EH, their molecular structures have been determined using single crystal X-ray analysis and compared to those of related 1H-perimidine derived species. The crystal packings from the solid-state structures of 1C, $1C^+I^-$, and 1CH were compared and revealed further stability of the molecule 1C through intermolecular N[sbnd]H···N hydrogen bonding and π···π stacking interactions, while in the case of molecules $1C^+I^-$, and 1CH through short interatomic C[sbnd]H···C contacts between two adjacent perimidine rings. To further quantify the intermolecular interactions and investigate their contributions to the crystal packing in each molecule, Hirshfeld surface analysis was performed. The redox properties of the perimidinium salts $1A^+I^-$–$1F^+I^-$, and the hydride reduced species 1AH–1FH were studied using cyclic voltammetry, and compared to that of N-DMBI-H ((4-(1,3-dimethyl-2,3-dihydro-1H-benzo[d]imidazole-2-yl)phenyl)dimethylamine). The salts exhibit an irreversible reduction wave, like those of 2-substituted-1,3-dimethyl-1H-benzo[d]imidazolium salts, while the hydrides undergo a reversible oxidation process, with the peak ratio (I_{pc}/I_{pa}) > 0.5. This shows the chemical stability of the $1H^{\bullet+}$ species at a scan rate of 100 mV s^{-1}.

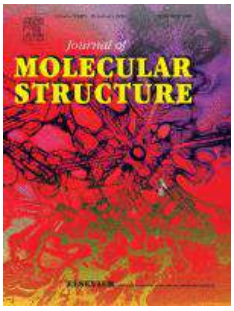

URL: https://www.sciencedirect.com/science/article/abs/pii/S0022286023020100?via%3Dihub

Journal Name: Physica E: Low-Dimensional Systems and Nanostruct **IF: 3.3**

Title: Effect of NM (B, C, N, O and F) doping and Feâ€“NM co-doping on structure, electronic and magnetic properties of monolayer 2Hâ€“MoTe2 : A first principle investigation

Author: Anagha G., Anjan Kumar Jena & Jyoti Mohanty

Details: Volume 156, January 2024

Abstract: Exploring magnetism in two-dimensional transition-metal dichalcogenides (TMDs) has gained a plethora of interest in recent times. Herein, employing spin-polarized density functional theory, we looked into the effect of non-metal doping (B, C, N, O, and F) and Fe-non metal co-doping on structure, electronic, and magnetic properties of 2H–$MoTe_2$ to identify new promising configurations for spin-based device applications. For non-metal doping, the results depict that B, N, and F-doped systems are magnetic, and the N-doped system shows magnetic-semiconducting behavior. The half-metallic Fe-doped $MoTe_2$ transforms into a magnetic semiconductor upon co-doping. The structural distortion around the Fe atoms modifies the crystal field splitting, resulting in triply degenerate a_1 and singly degenerate a_2 and a_3 states. Uncompensated electrons in the co-doped system and hybridization between Fe and NM atom modifies the magnetic properties of monolayer $MoTe_2$. Competition between crystal field splitting and intra-atomic Hund's exchange splitting determines the magnetic moment. Due to charge compensation, C-doped and Fe–C co-doped systems are non-magnetic. N-doped and Fe–N co-doped $MoTe_2$ exhibit long-range magnetic ordering. Formation energy calculations revealed that the co-doped configurations are easily attainable in experiments compared to non-metal doped systems. The results open up a robust way to realize 2H–$MoTe_2$ based spintronic devices. reversible oxidation process, with the peak ratio (I_{pc}/I_{pa}) > 0.5. This shows the chemical stability of the $1H^{\bullet+}$ species at a scan rate of 100 mV s^{-1}.

URL: https://www.sciencedirect.com/science/article/pii/S1386947723001960?via%3Dihub

Journal Name: Polymer Bulletin **IF: 3.2**

Title: A clinical perspective of chitosan nanoparticles for infectious disease management

Author: Dilnawaz, Fahima; Acharya, Sarbari; Kanungo, Anwesha

Details: Volume 81, Issue 2, 2024, Page 1071–1095

Abstract: Infectious diseases and their effective management are still a challenge in this modern era of medicine. Diseases, such as the SARS-CoV-2, Ebola virus, and Zika virus, still put human civilization at peril. Existing drug banks, which include antivirals, antibacterial, and small-molecule drugs, are the most advocated method for treatment, although effective but they still flounder in many instances. This calls for finding more effective alternatives for tackling the menace of infectious diseases. Nanoformulations are progressively being implemented for clinical translation and are being considered a new paradigm against infectious diseases. Natural polymers like chitosan are preferred to design nanoparticles owing to their biocompatibility, biodegradation, and long shelf-life. The chitosan nanoparticles (CNPs) being highly adaptive delivers contemporary prevention for infectious diseases. Currently, they are being used as antibacterial, drug, and vaccine delivery vehicles, and wound-dressing materials, for infectious disease treatment. Although the recruitment of CNPs in clinical trials associated with infectious diseases is minimal, this may increase shortly due to the sudden emergence of unknown pathogens like SARS-CoV-2, thus turning them into a panacea for the management of microorganisms. This review particularly focuses on the all-around application of CNPs along with their recent clinical applications in infectious disease management.

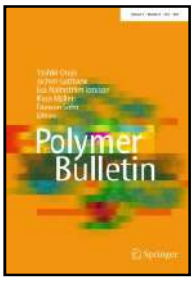

URL: https://link.springer.com/article/10.1007/s00289-023-04755-z

Journal Name: Optical and Quantum Electronics **IF: 3.0**

Title: New wave dynamics of the time-fractional Kaup–Kupershmidt model of seventh-order arises in shallow water waves

Author: A. Tripathy & S. Sahoo

Details: Volume 56, Article number 472, January 2024

Abstract: In this paper, a new variety of solitary wave patterns to the time-fractional seventh-order Kaup–Kupershmidt equation is studied. This model is important because of its nonlinear effects on the propagation of different water waves. For this study, we have considered the beta-fractional derivative form of the model. To derive the required exact solutions, we have used two analytical methods, specifically the new Kudryashov (nK) and modified Khater (mK) methods. Different types of wave patterns are produced from the solutions for distinct fractional and unidentified parameter values. These solutions include bright, two-soliton propagation, combined bright-dark, w-shaped pattern, combined dark-bright, m-shape wave, l-shaped bright wave, w-shaped periodic, u-shaped wave-form, and grey-type w-shaped periodic wave solutions. These dynamics of different wave natures are analyzed thoroughly by the graphical depiction of the solutions. Additionally, the characteristics of water waves and their many application areas can benefit greatly from these solutions such as surface waves in deep water, the dynamics of liquid-vapour interfaces, and many more. These solutions help us to understand how nonlinearity can affect the system during wave propagation. The novel aspect of this work is that the investigated model of the beta fractional form has never been solved before.

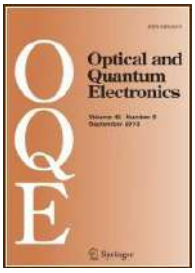

URL: https://link.springer.com/article/10.1007/s11082-023-05901-7

SCHOLARLY PUBLICATIONS
School of Applied Sciences
KIIT Deemed to be University

Journal Name: Physica Scripta **IF: 2.9**

Title: MHD second-grade nanofluid slip flow over a stretching sheet subject to activation energy, thermophoresis, and Brownian effects

Author: Rath C., Nayak A.

Details: Volume 99, Issue 3, 1 March 2024, Article number 035228

Abstract: In this work, the magnetohydrodynamic flow of two engine oil-based second-grade nanofluids Copper (Cu) and Titanium oxide (TiO_2) over a penetrable stretching sheet is studied. The flow, heat and mass transfer characteristics in the existence of activation energy, inclined magnetic field, Brownian diffusion, elastic deformation, and thermophoresis are examined. The coupled nonlinear model equations are formulated by implementing the Modified Buongiorno model and then are non-dimensionalized by the similarity transformation technique. The non-dimensional equations are simulated numerically using the bvp4c solver. Graphs are plotted to study the flow behaviour of nanofluid with the rate of entropy generation and Bejan number. The outcomes of skin friction coefficient, Nusselt number and Sherwood number are exhibited via surface plots. From the analysis, a higher inclination of the magnetic field decays the velocity and amplifies the temperature profiles. The heat transport rate diminishes with the Brownian diffusion, thermophoresis and elastic deformation parameters. The mass transport rate is accelerated due to the activation energy parameter. The entropy generation rate is enhanced with the Brinkman, Biot and local Reynolds numbers. Furthermore, it is seen that engine oil-based TiO_2 nanofluid has larger velocity, temperature and rate of entropy generation than engine oil-based Cu nanofluid. The current examination has applications in automobile radiators, microchips, biomedical engineering, and extraction of geothermal power.

URL: https://iopscience.iop.org/article/10.1088/1402-4896/ad2659

SCHOLARLY PUBLICATIONS
School of Applied Sciences
KIIT Deemed to be University

Journal Name: Journal of Materials Science: Materials in Electronics **IF: 2.8**

Title: Photocatalytic degradation of malachite green dye under solar light irradiation using ZnO and ZnO-TiO2 nanoparticles

Author: Nayak, Nibedita; Singha, Shuvendu; Maity, Jyoti Prakash; Rath, Pragyan Parimita; Sahoo, Trilochan; Sahoo, Tapas Ranjan

Details: Volume 35, Issue 4, February 2024

Abstract: The fast growth of human civilization with rapid industrialization causes severe detrimental effects, as a result, freshwater sources are depleting day by day threatening the future of human civilization to the water crisis. It is essential to preserve water by eliminating pollutants and conserving it. Dyes are one of such toxic pollutants which have been used in numerous industries like plastics, textiles, cosmetics, paper and pulp, leather, and food industries. The effectiveness of the photocatalytic removal of the dye malachite green was examined in the current study employing two distinct additives as photocatalysts: ZnO and ZnO–TiO2 nanoparticles. Nanosized ZnO and ZnO–TiO2 were prepared by utilizing microwave-assisted combustion and co-precipitation methods, respectively. The obtained metal oxide nanoparticles were characterized by XRD, FESEM, TGA, FTIR, and BET. The photocatalytic effects of the synthesized metal oxides were estimated in an aqueous solution by degrading malachite green (MG) dye. The dye solution with each metal oxide was subjected to irradiation under sunlight as well as UV light and monitored up to the stage of complete decolorization. The results indicated that ZnO–TiO2 exhibits the highest photocatalytic performance in comparison to ZnO and TiO2 nanoparticles in the presence of sunlight. Further, the effects of dose and pH variation were examined. The highest efficiency of the degradation of dye was found to be 92% at pH 5.8 under sunlight radiation.

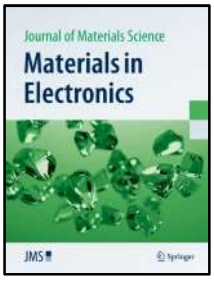

URL: https://link.springer.com/article/10.1007/s10854-024-12066-w

Journal Name: Applied Physics A: Materials Science & Processing **IF: 2.7**

Title: Influence of annealing on stability and regeneration of degraded CH3NH3PbI3 thin films

Author: Mohanty, Ipsita; Singh, Udai P.; Jana, Samaresh; Mangal, Sutanu

Details: Volume 130, Issue 2, February 2024

Abstract: In this study, wet chemical synthesis has been used to synthesize methyl ammonium lead iodide (CH3NH3PbI3). Spin-coating method has been employed to deposit CH3NH3PbI3 thin films of varying thicknesses on glass substrates. These samples were stored in vacuum desiccators and monitored over a 160-day period to investigate the degradation mechanism of perovskite thin films. To address the degradation issue, the degraded films were annealed at 70 °C for 30 min. During degradation, XRD data indicated a decrease in the intensity of CH3NH3PbI3 peaks and an increase in PbI2 peaks. After annealing, the intensity of CH3NH3PbI3 peaks was partially restored, but PbI2 was still present. Similarly, FESEM analysis revealed the presence of white, minute powder-like particles on the degraded samples and EDS data confirmed the presence of oxygen. However, the oxygen percentage decreased after annealing, and the white minute particles diffused. Subsequent analysis indicated that annealing partially restored the degraded films. Therefore, thermal annealing appears to be a possible solution to regenerate the degraded perovskite thin films.

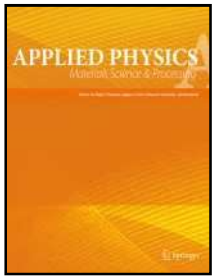

URL: https://link.springer.com/article/10.1007/s00339-023-07263-z

Journal Name: Fullerenes, Nanotubes and Carbon Nanostructures **IF: 2.3**

Title: Effect of oxidation temperature on Raman spectra of graphite samples

Author: Abdalrahman, Hiba; Kayed, Kamal; Alrefaee, Maher

Details: Volume 32, Issue 3, 2024, Pages 307-310

Abstract: The recent work investigates the relationship between the characteristics of the Raman spectra and the oxidation temperature of thermal-treated graphite samples in air at various temperatures ranging from 200°Cto 800 °C. Our findings indicate that thermal oxidation of graphite in air leads to the enhancement of the 2D vibration pattern while reducing the intensity of the D vibration pattern. Moreover, we report that chemical reduction begins at 550 °C. Furthermore, our results demonstrate that thermal oxidation causes a decrease in the disorder within the samples.

URL: https://www.tandfonline.com/doi/full/10.1080/1536383X.2023.2280229

SCHOLARLY PUBLICATIONS
School of Applied Sciences
KIIT Deemed to be University

Journal Name: Results in Chemistry **IF: 2.3**

Title: Enhanced electrochemical performance of in situ polymerized V2O5-PANI nanocomposites and its practical application confirmation by assembling ionic liquid as well as solid state-based supercapacitor device

Author: Thakur, Yugesh Singh; Acharya, Aman Deep; Sharma, Sakshi; Bisoyi, Sagar; Bhawna

Details: Volume 07, Article No. 101259, January 2024

Abstract: In the present study, in situ polymerization of anilinium hydrochloride over V2O5 was used to prepare PANI nanocomposites with varying weight percentage of V2O5 (10, 20 and 30 wt%). V2O5 nanoparticles were synthesized using a simple chemical approach and their purity was confirmed through Rietveld refinement. It confirmed the advantageous electrochemical activity of V2O5 with a higher oxidation state of vanadium (V+5), enabling efficient electron storage. For fabricated electrode materials, the pair of redox peaks as well as their shape in CV suggests the faradic pseudocapacitive properties. Among all prepared electrodes, 20 wt% V2O5-PANI (PV2) nanocomposite demonstrates maximum specific capacitance of 820.5 Fg−1 at a current density of 1 Ag−1 with decent capacitive retention of 88 % after 1000 charge–discharge cycles. PV2 electrode also has a lower charge transfer resistance (Rct) of 0.5 Ω and lesser solution resistance (Ro) of 0.31 Ω in 6 M KOH electrolyte which is also responsible for good electrochemical performance. The higher capacitance value and decent stability of PV2 confirmed its ordered structure with more active sites shown through FESEM, which significantly contributes to efficient ion and electron transfer. In addition, the symmetric supercapacitor configuration of PV2 electrodes exhibits good energy and power densities of 4.6 Wh kg−1 and 80.7 W kg−1, respectively. Finally, the ignition of a red LED using three PV2//PV2 symmetric devices connected in series underscores its potential to advance energy storage applications.

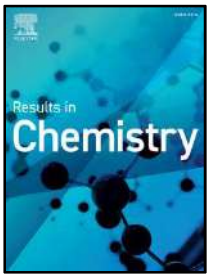

URL: https://www.sciencedirect.com/science/article/pii/S2211715623004988?via%3Dihub

Journal Name: European Journal of Inorganic Chemistry **IF: 2.3**

Title: Structural and Magnetic Properties of a {GdCu5}2 Metallacrown Dimer with a Disulfonate Linker

Author: Pavlishchuk, Anna V.; Zeller, Matthias; Carrella, Luca M.; Rentschler, Eva; Bindra, Jasleen K.; Dalal, Naresh; Kinyon, Jared; Perera, Kuluni; Pavlishchuk, Vitaly V.; Addison, Anthony W.

Details: Volume 1296 Part 1, Article No. 136920, January 2024

Abstract: The complex {Na2(H2O)8[GdCu5(GlyHA)5(H2O)4L]2}L2 · 2.5DMF · 10.5H2O (1, where GlyHA2−= glycinehydroxamate, L2−= 4,4′-bis(2-sulfonatostyryl)biphenyl) was obtained as the outcome of the metathesis reaction of previously reported [GdCu5(GlyHA)5(CO3)(NO3)(H2O)5] · 3.5H2O with an excess of the disulfonate's sodium salt. X-Ray analysis of 1 shows a dimeric structure in which 15-metallacrown-5 units {GdCu5}3+ are arranged in an "edge-to-edge" manner by way of two linking disulfonates, L2−. Magnetic studies of polycrystalline 1 over a temperature range of 2–300 K revealed both Gd-Cu ferromagnetic and Cu-Cu antiferromagnetic interactions within the metallacrown unit. Experimental χMT vs. T data for 1 were fitted using different theoretical models. A two-J model, which takes into account both exchange interactions between adjacent copper(II) ions and the Gd-Cu exchange interactions allows fitting of the χMT vs. T data in the whole temperature range. The values obtained for the exchange parameters are in accord with previously reported parameters for Ln(III)-Cu(II) 15-metallacrowns-5. The 240 GHz powder EPR spectra for 1 were recorded between 30 and 150 K.

URL: https://chemistry-europe.onlinelibrary.wiley.com/doi/10.1002/ejic.202300544

Journal Name: Journal of Applied Mathematics and Computing **IF: 2.2**

Title: Additive conjucyclic codes over a class of Galois rings

Author: Islam, Habibul; Bhunia, Dipak Kumar

Details: Volume 70, 2024, Pages 235-250

Abstract: As a tool towards quantum error correction, additive conjucyclic codes have gained great attention. But, their algebraic structure is completely unknown over finite fields (except F-q2) as well as rings. In this article, we investigate the structure of additive conjucyclic codes over Galois rings GR(2(r), 2), where r >= 2 is an integer. We develop a one-to-one correspondence between the family of additive conjucyclic codes of length n over GR(2(r), 2) and the family of linear cyclic codes of length 2n over Z(2r). This correspondence helps to obtain additive conjucyclic codes over GR(2(r), 2) via known linear cyclic codes over Z(2r). We prove that the trace dual C Tr of an additive conjucyclic code C is also an additive conjucyclic code. Moreover, we derive a necessary and sufficient condition of additive conjucyclic codes to be self-dual. We further propose a technique for constructing linear cyclic codes over Z(2r) contained in additive conjucyclic codes over GR(2(r), 2). Last but not least, we explicitly derive the generator matrices for these codes.

URL: https://link.springer.com/article/10.1007/s12190-023-01962-9

SCHOLARLY PUBLICATIONS
School of Applied Sciences
KIIT Deemed to be University

Journal Name: AIMS Mathematics **IF: 2.2**

Title: Numerical treatment for time fractional order phytoplankton-toxic phytoplankton-zooplankton system

Author: Priyadarsini D., Sahu P.K., Routaray M., Chalishajar D.

Details: Volume 9, Issue 2, Pages 3349 – 3368, 2024

Abstract: The study of time-fractional problems with derivatives in terms of Caputo is a recent area of study in biological models. In this article, fractional differential equations with phytoplankton-toxic phytoplankton-zooplankton (PTPZ) system were solved using the Laplace transform method (LTM), the Adomain decomposition method (ADM), and the differential transform method (DTM). This study demonstrates the good agreement between the results produced by using the specified computational techniques. The numerical results displayed as graphs demonstrate the accuracy of the computational methods. The approaches that have been established are thus quite relevant and suitable for solving nonlinear fractional models. Meanwhile, the impact of changing the fractional order of a time derivative and time t on populations of phytoplankton, toxic-phytoplankton, and zooplankton has been examined using graphical representations. Furthermore, the stability analysis of the LTM approach has been discussed.

URL: https://www.aimspress.com/article/doi/10.3934/math.2024164?viewType=HTML

Journal Name: Indian Journal of Physics **IF: 2.0**

Title: Equilibrium points and their linear stability analysis under the effect of dark matter halo

Author: Mia R., Nayak S.P., Tiwary R.D.

Details: 13 February 2024

Abstract: The motion of a test particle is studied under the influence of the gravitational force from the primaries and the force due to dark matter halo. To investigate the motion, we have modified the restricted three-body problem in which an additional potential from the dark matter halo is considered. We have obtained the locations of collinear and triangular equilibrium points semi-analytically. The linear stability of triangular equilibrium points is studied. The critical mass is obtained which is important for the stability analysis. The variations of critical mass parameter are shown with respect to the different parameters. Moreover, we have obtained the orbits around the triangular equilibrium points and it is found that the motion around the triangular points is oscillatory and bounded.

URL: https://link.springer.com/article/10.1007/s12648-024-03097-4

Journal Name: International Journal of System Assurance Engineering and Management **IF: 2.0**

Title: Fifth step block method and shooting constant for third order nonlinear dynamical systems

Author: Jena S.R., Sahu I., Paul A.K.

Details: 13 February 2024

Abstract: In this paper, the approximate solution of a set of nonlinear third order differential equations with mixed boundary conditions is obtained by employing the fifth step block method and Modified Taylor Series Scheme (MTSS). The motivation of this subject to implement MTSS for determining the shooting constants associated with the Initial Value Problems (IVPs) rather than Boundary Value Problems (BVPs). The fifth step block method is also used to solve nonlinear third Order Differential Equations (ODEs) on the definite interval. Two numerical examples are experimented to demonstrate the efficiency and accuracy of the proposed scheme by obtaining the absolute errors. Furhter, the order, convergence and stability of the proposed method are discussed to strengthen the theoretical concept.

URL: https://link.springer.com/article/10.1007/s13198-023-02237-z

Journal Name: Transactions on Electrical and Electronic Materials **IF: 1.9**

Title: Study of Variation in Optical Properties and Dispersion Parameters of Fe-Doped TiO2 Nanopowders

Author: Apta, Debabandana; Das, Susanta Kumar; Devi, Maya

Details: Volume 25, Issue 1, 2024, Pages 59-66

Abstract: TiO2 and Fe-doped TiO2nanopowders with (4 and 8wt.% of Fe doping) are synthesized by using the sol–gel technique starting from powder precursor. The optical properties of the prepared samples are investigated in the wavelength range of 200–800 nm.The refractive indices and extinction coefficients are calculated from the reflectance data using the Kramers-Kronigrelation. 4wt.% Fe doped sample has minimum refractive index value in comparison to others. The variation in refractive index value is studied using a single oscillator Wemple and Di Domenico model fitting and the optical parameters like oscillator energy, dispersion energy, and carrier concentration are evaluated and their variations are studied with doping concentration.

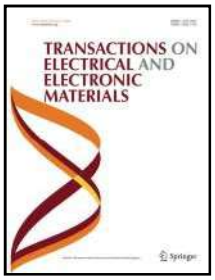

URL: https://link.springer.com/article/10.1007/s42341-023-00482-4

Journal Name: Afrika Matematika **IF: 1.1**

Title: The L-fuzzy cover spaces and L-fuzzy compact open topology

Author: Routaray, M.

Details: Volume 35, Issue 1,January 2024

Abstract: In this paper, a new concept of L-fuzzy cover spaces regarding fuzzy topological spaces is added. Secondly, the ideas of L-fuzzy compact open topology is established and the number of their interesting properties are studied.

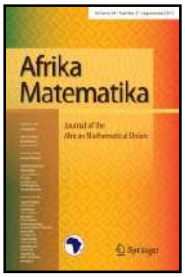

URL: https://link.springer.com/article/10.1007/s13370-023-01158-1

Journal Name : Linear and Multilinear Algebra **IF: 1.1**

Title: A remark on the spectrum of fractional difference operator

Author: Patra A., Baliarsingh P., Nayak L.

Details: Volume 72, Issue 1, Pages 50 – 58, 2024

Abstract: This work computes the spectrum of the backward fractional difference operator (Formula presented.) (Formula presented.) over various Banach spaces (Formula presented.) and (Formula presented.). Note that recently, the spectrum of the fractional difference operator (Formula presented.), ((Formula presented.) being either a constant or strictly decreasing sequence of positive real numbers satisfying some conditions) on the sequence space (Formula presented.) has been computed by Baliarsingh P. [On the spectrum of fractional difference operator. Linear Multilinear Algebra. 2021;1–13] and it has been noticed that the results obtained are unified and more general, but lack of accuracy for the case (Formula presented.). In this work, we improve the results by providing the sharper estimations and some illustrative examples. Also, individual sets describing the point, the residual and the continuous spectrum of the operator (Formula presented.) on the Banach space c and (Formula presented.) are computed.

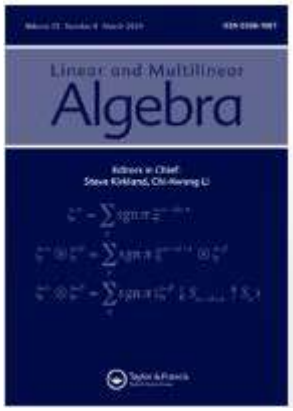

URL: https://www.tandfonline.com/doi/full/10.1080/03081087.2022.2155795

Journal Name : Materials Science and Engineering: B **IF: 1.08**

Title: Negative temperature co-efficient of resistance behaviour of Cr doped ZnO nanoceramics

Author: Das B.K., Das T., Das D., Parashar K., Parashar S.K.S., Kumar R., Anupama A.V., Sahoo B.

Details: Volume 299, January 2024, Article number 117017

Abstract: Here, High Energy Ball Milling (HEBM) is used to prepare Cr doped ZnO ($Zn_{1-x}Cr_xO$, x = 0–0.04) nanoceramics and their electrical behaviour is studied in detail. The X-ray diffraction suggests a hexagonal wurtzite structure. The Rietveld refinement XRD pattern of the sample calcined at 900 °C suggests that up to 4 at% of Cr can be doped into the ZnO structure. After sintering, the growth in the particle size was observed for Cr doped ZnO samples. The complex impedance behaviour of samples suggests a decrease in resistance with temperature. This shows the Negative Temperature Coefficient of Resistance (NTCR) characteristic of the Cr doped ZnO sample in the studied temperature range (300–500 °C). At higher temperature, the electrical relaxation behaviour is of the non-Debye type as observed from the relaxation time distribution. The equivalent electrical circuit of ZnO and Cr doped ZnO ceramic samples are a parallel arrangement of bulk capacitance (C_b) and bulk resistance (R_b).

URL: https://www.sciencedirect.com/science/article/pii/S0921510723007596